WORLD JOURNAL OF PHARMACEUTICAL RESEARCH
SJIF Impact Factor 7.523
Volume 2, Issue 2, 511-521. Research Article ISSN 2277– 7105

EU(III) CHELATE COMPLEXES AND THEIR LUMINESCENT PROPERTIES

***Mir Shabeer Ahmad**

*Govt. Degree College Kulgam Jammu & Kashmir (India).

Article Received on
18 Jan. 2013,
Revised on 08 Feb. 2013,
Accepted on 28 Feb. 2013
DOI: 10.20959/wjpr20132-8632

***Corresponding Author**
Mir Shabeer Ahmad
Govt. Degree College
Kulgam Jammu & Kashmir
(India).

ABSTRACT

The silver rods were fabricated in a seed-growth method followed by depositing thin layers of silica on the surfaces. The europium chelates were physically absorbed in the silica layers on the silver rods. The silver rods were observed to exhibit two plasmon absorption bands from longitudinal and transverse directions, respectively, centered at 394 and 675 nm, close to absorption and emission bands from the Eu(III) chelates. As a result, the immobilized Eu(III) chelates on the silver rods should have strong interactions with the silver nanorods and lead to greatly improved optical properties. The Eu–Ag rod complexes were observed to have enhanced emission intensity up to 240-fold in comparison with the Eu(III) chelates in the metal-free silica templates. This enhancement is much larger than the value for the Eu(III) chelates on the gold rods or silver spheres indicating the presence of stronger interactions for the Eu(III) chelates with the silver rods. The interactions of Eu(III) chelates with the silver rods were also proven by extremely reduced lifetime.

KEYWORDS: Silver, Chelates, Europium, Plasmon, Silica templates.

INTRODUCTION

It is known that a lanthanide emits luminescence with a large Stokes shift, narrow emission band, and long lifetime, so the use of lanthanide dyes may offer an opportunity to create a sensitive time-resolved bioassay or cell imaging with a low luminescence background.[1-2] However, the emission from the lanthanide may involve an electron transition in its 4f orbits, which is basically forbidden, so in comparison with a conventional organic fluorophore the lanthanide dye often has an extremely low absorbance coefficient and a very slow emissive rate.[3-4] Consequently, the lanthanide dye often displays a low quantum yield and brightness, and a lanthanide-based fluorescence bioassay often results in a low detection sensitivity. In

addition, the lanthanide dye has an extremely long decay time up to milliseconds, which may often bring up a low photon count rate in the emission and result in low emission intensity. Therefore, the single molecule detection (SMD) of the lanthanide dye is not reported to date.[5-6]

With advances in coordination chemistry, new lanthanide chelates have been developed with significantly improved optical properties.[7] Basically, these lanthanide chelates are created by coordinating chromophores with lanthanide ions, in which the chromophores can act as antennas or sensitizers to absorb photons and subsequently transfer the photons to the lanthanide centers for increasing their emission rates and efficiencies. In comparison with the lanthanide ions, these lanthanide chelates have significantly increased optical properties including brightness and quantum yields. Because of absorption from the ligands, the lanthanide chelates often exhibit a broader excitation range leading to a significant shift of maximal excitation wavelength to the red region.[5] Hence, it is believed that the formation of lanthanide chelates may overcome some inherent weakness of lanthanide dyes especially on the absorption cross-section and excitation wavelength. However, it is also noticed that the decay rate of the lanthanide center in the chelate is not really increased with the coordination.[6] Therefore, there is a basic research need to develop a strategy that can increase the radiative rate of the lanthanide chelate and furthermore increase the cyclic number for the excitation/emission of Eu(III) chelate in a period of time and the photon count rate in the measurement.

The near-field interaction approach is considered to enable use for such a purpose. Fundamentally, as induced by an incident light, the metal nanoparticle of subwavelength size can create a local electric field around it.[8-9] When a fluorophore is put in the local field within a near-field range from the metal nanoparticle, the coupling interaction between the fluorophore and metal nanoparticle can increase the radiative rate of the fluorophore and furthermore enhance the emission intensity of the fluorophore up to 10- to 10^3-fold.[10-11] Increased radiative rate of the fluorophore may also bring a decrease in the lifetime.[12] Thus, the metal-enhanced fluorescence (MEF) by the near-field interaction effect is often accompanied with a decrease of lifetime for a fluorophore. In this study, the near-field interaction approach was employed to improve the optical properties of lanthanide chelates. Typically, the lanthanide chelates were immobilized on the metal nanoparticles within a near-field range to initiate the coupling interactions. The feasibility of this approach has been

demonstrated by one of our earlier reports in which the lanthanide chelates were localized in the cores of silver shells and the emission could be greatly enhanced due the near-field interactions.[13] More work is needed to optimize the conditions for achieving maximally enhanced luminescence.[14-15]

Metal nanorods have been widely reported as new nanoparticle substrates.[16] We were interested in the metal rods and intended to use them as the substrates to couple with the lanthanide chelates because the metal rods can display two separated plasmon bands from the longitudinal and transverse directions, respectively, and the band maxima can be tuned with the aspect ratio of metal rods.[17-18] Particularly, we have research interest in silver nanorods because the silver rods can display two plasmon bands close to the absorption and emission maxima from the Eu(III) chelates. In this study, the silver rods were fabricated in a chemical method followed by depositing the silica layers on the surfaces. The Eu(III) chelates were physically absorbed in the silica layers on the silver rods within the near-field range from the metal surfaces. Optical properties from the Eu(III) chelates on the silver rods were determined on an ensemble fluorescence spectrophotometer with the time-gated conditions. Compared with the emission properties of Eu(III) chelates in the metal-free silica templates, the influences from the silver rods to the emission of Eu(III) chelates could be explored. The gold rods and silver spheres were also fabricated and immobilized with the Eu(III) chelates in the same strategy. The optical properties from the Eu–Au rod and Eu–Ag sphere complexes were determined as controls of the properties on the silver rods.

Experimental section

All reagents and spectroscopic grade solvents were used as received from Fisher or Sigma/Aldrich. Tris-(dibenzoylmethanate)mono(5-amino-1,10-phenanthroline) europium chelates were commercially available from Sigma/ Aldrich. Nanopure water (>18.0 $M\Omega \cdot cm^{-1}$) purified on a Millipore Milli-Q gradient system was used in all experiments.

Preparation of Metal Nanorods

In a modified seed growth method, the silver nanorods were fabricated in aqueous solutions with a defined aspect ratio.[19-20] In brief, small silver nanoparticles were first generated as a seed solution to initiate the growth of silver rods. Typically, 20 mL aqueous solution with 0.25 mM $AgNO_3$ and 0.50 mM sodium citrate was added by 1 mL of ice-cold 0.1 M $NaBH_4$ solution with rigorous stirring. The color of solution was turned to yellow representing the formation of small silver nanoparticles, which had an average diameter of 4

nm. For the silver rod fabrication, 10 mL of aqueous solution with 0.25 mM $AgNO_3$, 80 mM cetryltrimethylammoium bromide (CTAB), and 0.5 mM ascorbic acid were added to a 30 µ*L* seed solution. The mixing solution was continuously stirred for 30 min. The color of the solution changed from yellow to green representing the formation of silver rods. The formed silver rods were collected by centrifugations followed by dispersing in 1 mL of mixing solvent of water/ethanol (v/v = 1) for depositing the silica layers on the external surfaces.

Depositing Silica Layers on Metal Nanoparticles

In a modified Stöber method, thin silica layers were deposited on the metal nanoparticles including silver rods, gold rods, and silver spheres for immobilizing the europium chelates[21-22] Typically, 1 mL of metal nanoparticle solution was added by 1 mL of water/ethanol (v/v = 1) solution containing 1×10^{-3} M tetraethyl orthoorthosilicate. Subsequently, 10 µ*L* of 30% ammonia solution was added dropwise under vigorous stirring. The solution was stirred overnight at room temperature to form the silica layers on the metal nanoparticles. The suspension solution was removed by centrifugation and the residual solid was dispersed in 1 mL of a mixing solvent of *N*,*N*-dimethylformamide (DMF)/alcohol (v/v = 1/1) for immobilizing the europium chelates.

Immobilizing Eu(III) Chelates on Metal Nanoparticles

Tris(dibenzoylmethanate)mono(5-amino-1,10-phenanthroline) europium chelates were immobilized into the silica layers on the metal nanoparticles via physical absorptions.[23] The Eu(III) chelates (1×10^{-5} M) were codissolved in a mixing solution of DMF/alcohol (v/v = 1/1) containing the silica-treated metal nanoparticles (1×10^{-8} M). The solution was stirred for 12 h at room temperature, and the suspension was removed by centrifugation. The residual solid was subsequently washed with DMF, ethanol and water. The collected metal nanoparticles were dispersed in water for the ensemble spectral measurements.

Ensemble Spectral and Anisotropy Measurements

Absorption spectra were conducted on a Hewlett-Packard 8453 spectrophotometer. Ensemble fluorescence spectra were recorded with a Cary Eclipse Fluorescence Spectrophotometer. Because of a slow decay time of Eu(III) chelate, a time-gated technique was used to collect the emission from the lanthanide, in which the gate pulse width was 0.5 ms and the delay time was 0.1 ms. All Eu(III) chelate-associated samples were excited at 380 nm for their emission spectral collections. In the current measurements, the polarized emission of Eu(III) chelate-associated samples were determined with two orthogonal polarizations, one parallel

and one perpendicular to the excitation polarization vector.[24] The emission anisotropies of Eu(III) chelate-associated samples were determined in the single-channel method under the same time-gate conditions.

TEM Image

For the TEM measurements, the nanoparticle samples were diluted to nanomolar concentrations followed by casting onto the copper grids (200 mesh) with standard carbon-coated Formvar films (200–300 Å). The samples were dried in air. TEM images were taken with a side-entry Philips electron microscope at 120 keV. The distributions of nanoparticle sizes were analyzed with Scion Image Beta Release 2 on the base on at least 200 images.

RESULT AND DISCUSSION

In this study, the silver nanorods were fabricated in a modified seed growth method.[25-26] The achieved silver rods could be distinctly outlined by TEM images (part a of Figure 1) showing an average length of 80 nm and width of 18 nm. As a control, the gold rods were also fabricated in the similar strategy and outlined by TEM image showing an average length of 60 nm and width of 20 nm (part b of Figure 1). The aspect ratios of metal rods hence were estimated to be ca. 5 for the silver and ca. 3 for the gold. These metal rods were stabilized by cetryltrimethylammoium bromide (CTAB) on the surfaces. As expected, the metal rods exhibited distinct two plasmon absorption bands from the longitudinal and transverse directions, respectively, in aqueous solution (Figure 2), on which the bands from the silver rods were centered at 394 and 675 nm and the bands from the gold rods were centered at 536 and 982 nm. Tris(dibenzoylmethanate)mono(5-amino-1,10-phenanthroline) europium chelate was employed to immobilize on the metal rods for exploring the near-field interactions. It was observed that this Eu(III) chelate exhibited an absorption band and an emission band centered at 353 and 614 nm (Figure 3), respectively, close to the plasmon bands from the silver rods. Thus, there were sufficient spectral couplings between the Eu(III) chelates and silver rods at both the excitation and emission processes and as a result the Eu(III) chelates in the near-field range from the metal rods were expected to have strong interactions with the silver rods leading to greatly improved optical properties.

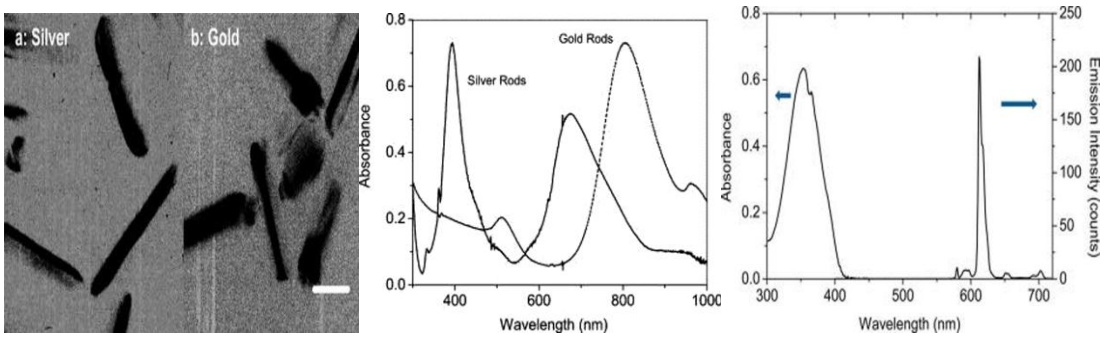

Fig 1. Low-resolution TEM images of (a) silver and (b) gold nanorods. The scale bar in the image is 20 nm.

Fig 2. Ensemble absorption spectra of silver and gold nanorods in aqueous solutions.

Fig 3 Ensemble absorption and emission spectra of Eu(III) chelate in dimethylformamide (DMF) solution. The emission spectrum was collected upon excitation at 380 nm. The gate pulse width was controlled to be 0.5 ms and the delay time was 0.1 ms.

The Eu(III) chelates were immobilized in the silica layers on the metal rods. Because the Eu(III) chelates were required to localize in the near-field range, the silica layers on the metal rods were thin. Typically, the metal rods were deposited by thin silica layers through a hydrolysis reaction of tetraethyl orthosilicate. By the ratio of orthosilicate monomer over the metal rod in the reaction solution, the silica layer on the metal rod was controlled to be ca. 5 nm thick. The silane-treated metal rods were dispersed in a mixed solvent of DMF/ alcohol containing Eu(III) chelates to absorb the Eu(III) chelates from solution by physical interactions . The Eu–metal rod complexes were recovered by configuration and dispersed in water for the spectral measurements. It was difficult to outline the silica layers from the metal rods on the TEM images because of their thin thickness. But they could be identified by the emission spectral measurements. For the silane-treated metal rods, there was significant luminescence detectable after absorbing the Eu(III) chelates, whereas for the untreated metal rods there was no luminescence after absorbing the Eu(III) chelates supporting that there were the silica layers formed on the metal rods after the silane-treatments. The Eu(III)–Ag rod complexes were observed to display two plasmon bands and the band maxima remained almost unchanged from those from the CTAB-coated silver rods, indicating the silver rods were chemically stable in the surfaces reactions. The Eu(III) chelates were immobilized on the metal rods but the immobilized Eu(III) chelate so the metal rods could not be determined by the absorption spectrum because of strong interference from the plasmon bands from the metal rods. Thus, the emission spectrum was used to determine the Eu(III) chelates on the

silver rods. It was shown that upon excitation at 380 nm the Eu(III)–Ag rod complexes displayed an emission band centered at 610 nm (Figure 4), a 4 nm shift to blue in comparison with the free Eu(III) chelates. The emission band from the Eu(III)–Ag rod complexes was also significantly broadened, which was primarily due to the restriction of the movements of Eu(III) chelates after they were immobilized in the solid templates as well as the structural heterogeneity of Eu(III) chelates in the nearby environments[27] In fact, it has been widely reported that the emission band becomes broadened with the immobilization of fluorophores into the solid substrates in comparison with that in solution. These fluorophores include not only lanthanide chelates but also many other organic fluorophores. The breakdown of beta-diketonate by the acidic conditions in the silica is also considered as a possible reason causing such broadness. But because there is no significant change in the emission spectrum except the broadness with the immobilization of Eu(III) chelates in the silica, we suggest that the restriction of movement for the immobilized fluorophore in the solid substrate and influence from the heterogeneous surrounding is still the primary reason causing such a change in the band broadness.

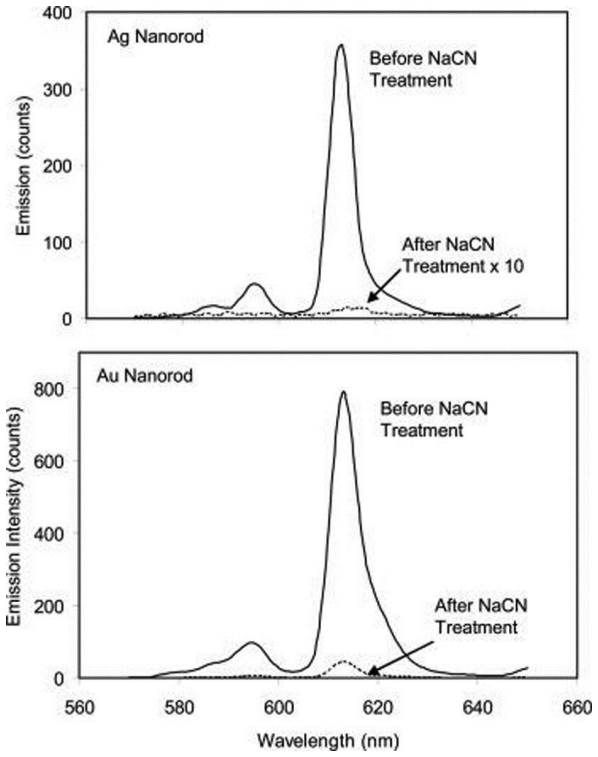

Fig. 5 Emission spectral changes for the Eu(III) chelates on the Ag rods and gold rods in aqueous solution prior to and after NaCN treatment. The emission spectra were collected upon excitation at 380 nm. The gate pulse width was controlled to be 0.5 ms and the delay time was 0.1 ms.

CONCLUSION

We studied the improved optical properties for the Eu(III) chelates on the metal nanorods due to the near-field interactions. The silver rods were fabricated in a wet chemical method followed by depositing thin silica layers on the surfaces. The Eu(III) chelates were followed by physically absorbing the silica layers on the silver rods. The silver rods displayed two plasmon bands, which had maxima close to the absorption and emission bands of the Eu(III) chelates. Thus, the Eu(III) chelates were expected to have strong interactions with the silver rods leading to greatly improved optical properties. The emission intensity could be enhanced up to 240-fold. Considering there were ca. 650 Eu(III) chelates on one silver rod, it was estimated that one Eu–Ag rod complex should be more than 1.5×10^5-fold brighter than one single free Eu(III) chelate. Because of the near-field interactions, the radiative rate of Eu(III) chelates on the silver rods is greatly increased leading to a dramatic decrease of lifetime from hundreds to several microseconds. However, this value is much longer than the lifetimes of most organic dyes, so the Eu–Ag rod complexes can be considered to use for time-resolved cellular assays.

REFERENCES

1. Binnemans K. Lanthanide-Based Luminescent Hybrid Materials. Chem. Rev. 2009; 109(4283): 4283–4374.
2. Bnzli J-CG. Lanthanide Luminescence for Biomedical Analyses and Imaging. Chem. Rev. 2010; 110: 2729–2755.
3. Moore EG, Samuel APS, Raymond KN. From Antenna to Assay: Lessons Learned in Lanthanide Luminescence. Acc. Chem. Res. 2009; 42: 542–552.
4. Sameiro M, Gonçalves T. Fluorescent Labeling of Biomolecules with Organic Probes. Chem. Rev. 2009; 109: 190–212.
5. Lakowicz JR. Principles of Fluorescence Spectroscopy. 3rd ed. New York: Kluwer Academic/Plenum Published; 2006.
6. Ma Y, Wang Y. Recent Advances in The Sensitized Luminescence of Organic Europium Complexes. Coord. Chem. Rev. 2010; 254: 972–990.
7. Yu J, Parker D, Pal R, Poole RA, Cann MJ. A Europium Complex That Selectively Stains Nucleoli of Cells. J. Am. Chem. Soc. 2006; 128: 2294–2299.
8. Halas NJ, Lal S, Chang W-S, Link S, Nordlander P. Plasmons in Strongly Coupled Metallic Nanostructures. Chem. Rev. 2011; 111: 3913–3961.

9. Giannini V, Fernandez-Domínguez AI, Heck SC, Maier SA. SA Plasmonic Nanoantennas: Fundamentals and Their Use in Controlling the Radiative Properties of Nanoemitters. Chem. Rev. 2011; 111: 3888–3912.
10. a) Lakowicz JR. Radiative Decay Engineering 5: Metal-Enhanced Fluorescence and Plasmon Emission. Anal. Biochem. 2005; 337: 171. b) Lakowicz JR. Radiative Decay Engineering: Biophysical and Biomedical Applications. Anal. Biochem. 2001; 298: 1–24.
11. Sokolov K, Chumanov G, Cotton TM. Enhancement of Molecular Fluorescence Near the Surface of Colloidal Metal Films. Anal. Chem. 1998; 70: 3898–3905. b) Ming T, Zhao L, Yang Z, Chen H, Sun L, Wang J, Yan C. Strong Polarization Dependence of Plasmon-Enhanced Fluorescence on Single Gold Nanorods. Nano Lett. 2009; 9: 3896–3903.
12. Morton SM, Silverstein DW, Jensen L. Heoretical Studies of Plasmonics Using Electronic Structure Methods. Chem. Rev. 2011; 111: 3962–3994.
13. a) Eichelbaum M, Rademann K. Plasmonic Enhancement or Energy Transfer? On the Luminescence of Gold-, Silver-, and Lanthanide-Doped Silicate Glasses and Its Potential for Light-Emitting Devices. Adv. Funct. Mater. 2009; 19: 2045–2052. (b) Nabika H, Deki S. Enhancing and Quenching Functions of Silver Nanoparticles on the Luminescent Properties of Europium Complex in the Solution Phase. J. Phys. Chem. B. 2003; 107: 9161–9164. (c) Selvan ST, Hayakawa T, Nogami M. Remarkable Influence of Silver Islands on the Enhancement of Fluorescence from Eu3+ Ion-Doped Silica Gels. J. Phys. Chem. B. 1999; 103: 7064–7067. (d) Malta OL, Santa-Cruz PA, De Sá GF, Auzel F. Fluorescence Enhancement Induced by the Presence of Small Silver Particles in Eu^{3+} Doped Materials. J. Lumin. 1985; 33: 261–272.
14. Blair S, Lowe MP, Mathieu CE, Parker D, Senanayake PK, Kataky R. Narrow-Range Optical pH Sensors Based on Luminescent Europium and Terbium Complexes Immobilized in a Sol Gel Glass. Inorg. Chem. 2001; 40: 5860–5867. (b) Zhang J, Fu Y, Lakowicz JR. Luminescent Silica Core/Silver Shell Encapsulated with Eu (III) Complex. J. Phys. Chem. C. 2009; 113: 19404–19410.
15. a) Enderlein J. Spectral Properties of A Fluorescing Molecule within A Spherical Metallic Nanocavity. Phys. Chem. Chem. Phys. 2002; 4: 2780–2786. (b) Enderlein J. Theoretical Study of Single Molecule Fluorescence in A Metallic Nanocavity. Appl. Phys. Lett. 2002; 80: 315–317.
16. Zhang J, Fu Y, Chowdhury M, Lakowicz JR. Single-Molecule Studies on Fluorescently Labeled Silver Particles: Effects of Particle Size. J. Phys. Chem. C. 2008; 112: 18–26.

17. Jain P, Huang K, El-Sayed X, El-Sayed IH, Noble MA. Metals on the Nanoscale: Optical and Photothermal Properties and Some Applications in Imaging, Sensing, Biology and Medicine. Acc Chem. Res. 2008; 41: 1578–1586.
18. Rycenga M, Cobley CM, Zeng J, Li W, Moran CH, Zhang Q, Qin D, Xia Y. Controlling the Synthesis and Assembly of Silver Nanostructures for Plasmonic Applications. Chem. Rev. 2011; 111: 36693712.
19. Schwartzberg AM, Zhang JZ. Novel Optical Properties and Emerging Applications of Metal Nanostructures. J. Phys. Chem. C. 2008; 112: 10323–10337.
20. Fang X, Cao Z, Beck T, Tan W. Molecular Aptamer for Real-Time Oncoprotein Platelet-Derived Growth Factor Monitoring by Fluorescence Anisotropy. Anal. Chem. 2001; 73: 5752–5257.
21. Deprez E, Tauc P, Leh H, Mouscadet JF, Auclair C, Brochon JC. Oligomeric States of the HIV-1 Integrase as Measured by Time-Resolved Fluorescence Anisotropy. Biochemistry. 2000; 39: 9275–9284.
22. Eriksson O, Brooks MSS, Johansson B. Orbital Polarization in Narrow-Band Systems: Application to Volume Collapses in Light Lanthanides. Phys. Rev. B. 1990; 41: 7311–7314.
23. Bunzli J-CG, Piguet C. Taking Advantage of Luminescent Lanthanide Ions. Chem. Soc. Rev. 2005; 34: 1048–1077.
24. a) Seitz M, Moore EG, Ingram AJ, Muller G, Raymond KN. Enantiopure, Octadentate Ligands as Sensitizers for Europium and Terbium Circularly Polarized Luminescence in Aqueous Solution. J. Am. Chem. Soc. 2007; 129: 15468–15470. (b) Blanc J, Ross DL. Polarized Absorption and Emission in an Octacoordinate Chelate of Eu^{3+}. J. Chem. Phys. 1965; 43: 1286–1289.
25. Galyametdinov YG, Knyazev AA, Dzhabarov VI, Cardinaels T, Driesen K, Görller-Walrand C, Binnemans K. Polarized Luminescence from Aligned Samples of Nematogenic Lanthanide Complexes. Adv. Mater. 2008; 20: 252–257. (b) Driesen K, Vaes C, Cardinaels T, Goossens K, Görller-Walrand C, Binnemans K. Polarized Luminescence of Non-mesogenic Europium-(III) Complexes Doped into a Nematic Liquid Crystal. J. Phys. Chem. B. 2009; 113: 10575–10579.
26. Hasegwa M, Ishii A, Furukawa K, Ohtsu H. Polarized ff-Emission of Terbium(III) by Using the Stretched Polymer Film Technique. J. Photopolym. Sci. Technor. 2008; 21: 333–338. (b) Wu S, Yu X, Huang J, Shen J, Yan Q, Wang X, Wu W, Luo Y, Wang K, Zhang Q. Optically Controllable Polarized Luminescence from Azopolymer Films Doped

with A Lanthanide Complex. J. Mater. Chem. 2008; 18: 3223–3229. (c) Srdanov VI, Robinson MR, Bartl MH, Bu X, Bazan GC. Polarization Effects of A Europium Complex in Stretched Polyethylene. Appl. Phys. Lett. 2002; 80: 3042–3044. (d) Yang CY, Srdanov V, Robinson MR, Bazan GC, Heeger AJ. Orienting $Eu(dnm)_3$ phen by Tensile Drawing in Polyethylene: Polarized Eu^{3+} Emission. Adv. Mater. 2002; 14: 980–983.

27. Lu L, Wang L-L, Zou C-L, Ren X-F, Dong C-H, Sun F-W, Yu S-H, Guo G-C. Doubly and Triply Coupled Nanowire Antennas. J. Phys. Chem. C. 2012; 116: 23779–23784. (b) Murphy CJ, Sau TK, Gole AM, Orendorff, Cuo J, Gao J, Gou L, Hunyadi SE, Li T. Anisotropic Metal Nanoparticles: Synthesis, Assembly, and Optical Applications. J. Phys. Chem. B. 2005; 109: 13857–13870.
28. Jana NR, Gearheart L, Murphy CJ. Wet Chemical Synthesis of Silver Nanorods and Nanowires of Controllable Aspect Ratio. Chem. Commun. 2001; 617–618.